

Cite this: *Dalton Trans.*, 2021, **50**, 8297Received 30th April 2021,  
Accepted 19th May 2021

DOI: 10.1039/d1dt01437d

rsc.li/dalton

# Iodonium complexes of the tertiary amines quinuclidine and 1-ethylpiperidine†

Jas S. Ward, \*<sup>a</sup> Antonio Frontera <sup>b</sup> and Kari Rissanen \*<sup>a</sup>

**Iodonium complexes incorporating tertiary amines have been synthesised to study and explore why such species comprised of alkyl amines are relatively rare. The complexes were characterised in solution (<sup>1</sup>H and <sup>15</sup>N NMR spectroscopy) and the solid state (SCXRD), and analysed computationally.**

Halonium ions, [L–X–L]<sup>+</sup> (X = Cl, Br, I), the acute case of a halogen atom that has been completely ionised to a formally cationic state, X<sup>+</sup> (termed a *halonium* ion),<sup>1</sup> and stabilised by a pair of Lewis bases (L), were first reported in the 1960s.<sup>2,3</sup> The utility of halonium complexes is well established, in large part due to the contributions of Barluenga from the 1990s onwards, who popularised them through a myriad of organic transformations such as the electrophilic iodination of unactivated arenes, the promotion of C–C and C–X bond formation, and the selective direct iodination of peptides.<sup>4–7</sup> This utility, coupled with their novelty as *relatively* stable examples of 2-coordinate halogen atoms in the unusual +1 oxidation state, has fuelled continued research on halonium ions.

Halonium ions can be readily prepared upon reaction with elemental halogens, X<sub>2</sub> (X = Br, I), *via* cation exchange from their respective silver(i) complexes (Scheme 1).<sup>8</sup> Directly combining a suitable nucleophilic base with X<sub>2</sub> can also yield a halonium motif, [X(L)<sub>2</sub>]X, although this pathway is more susceptible to side reactions due to the lack of a strong driving force (such as with the previously discussed pathway that precipitates AgX). Examples of halonium complexes in the literature are predominantly comprised of aromatic N-heterocycles (*e.g.*, pyridine), with few examples incorporating tertiary amines as the stabilising Lewis base,<sup>9–16†</sup> several of which were synthesised unintentionally. As a consequence, these ter-

tiary amine iodonium complexes have never been comprehensively studied in detail by modern analytical techniques. Given the recent slew of revelations in halonium chemistry with the first unrestrained heteroleptic,<sup>17–19</sup> supramolecular,<sup>15,20–23</sup> and nucleophilic interactions of iodonium complexes being reported,<sup>1,24,25</sup> renewed interest in halonium ions comprised of tertiary amines is warranted.

The tetrafluoroborate bromonium (Br<sup>+</sup>) and iodonium (I<sup>+</sup>; [1]BF<sub>4</sub>) solid-state structures of quinuclidine (quin) were reported in the 1980s;<sup>12,13</sup> however, no solution state data were included in either instance. Therefore, this was taken as an opportunity to access and expand this research, as a series of quinuclidine complexes with differing anions were also synthesised to explore any effects this change might have.

The addition of two equivalents of quin to a series of silver (i) salts, followed by cation exchange with elemental iodine, yielded the desired iodonium ion, [I(quin)<sub>2</sub>]<sup>+</sup> (**1**), with a range of anions ([1]BF<sub>4</sub>, [1]PF<sub>6</sub>, [1]NO<sub>3</sub>, and [1]ClO<sub>4</sub>) in quantitative yields, as determined by <sup>1</sup>H NMR spectroscopy. No apparent anion effects were observed in the solution state, with the <sup>1</sup>H and <sup>15</sup>N NMR chemical shifts for the four complexes being found to be effectively identical; therefore, [1]PF<sub>6</sub> is discussed as a representative of the series.

Upon complexation from uncoordinated quinuclidine to [1]PF<sub>6</sub>, three peaks in the <sup>1</sup>H NMR spectra were observed to shift to higher values by 0.46 ppm (α-H), 0.25 ppm (β-H), and 0.23 ppm (γ-H) (Fig. 1), a trend consistent with the reported NMR data of aromatic iodonium complexes.<sup>18</sup> However, the <sup>15</sup>N NMR spectra revealed that the quinuclidine resonance (–366.6 ppm) shifted in [1]PF<sub>6</sub> (–357.3 ppm) by 9.3 ppm. This

<sup>a</sup>University of Jyväskylä, Department of Chemistry, Jyväskylä 40014, Finland.

E-mail: james.s.ward@jyu.fi, kari.t.rissanen@jyu.fi

<sup>b</sup>Department of Chemistry, Universitat de les Illes Balears, Crts de Valldemossa km 7.6, 07122 Palma de Mallorca (Balears), Spain

†Electronic supplementary information (ESI) available: Synthesis, NMR and computational details. CCDC 2079430–2079434 and 2084411. For ESI and crystallographic data in CIF or other electronic format see DOI: 10.1039/d1dt01437d



**Scheme 1** A general method to synthesise halonium ions, facilitated by the strong driving force of the precipitation of AgX (spectator anions omitted for clarity).



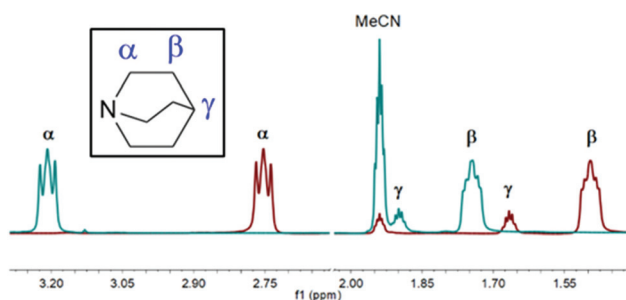


Fig. 1 The superimposed  $^1\text{H}$  NMR spectra (500 MHz, 298 K) in  $\text{CD}_3\text{CN}$  of quinuclidine (red) and  $[1]\text{PF}_6$  (turquoise) showing the observed shift upon formation of the iodonium complex. Inset: An annotated molecule of quinuclidine.

is of interest for two reasons: firstly, the change in the chemical shift is relatively small compared to previously reported aromatic iodonium complexes such as  $[\text{I}(\text{DMAP})_2]\text{PF}_6$  (DMAP = 4-dimethylaminopyridine). Upon complexation from uncoordinated DMAP ( $-107.2$  ppm) to  $[\text{I}(\text{DMAP})_2]\text{PF}_6$  ( $-216.1$  ppm), a difference of 108.9 ppm has been observed, and larger differences in the corresponding chemical shifts have been reported for heteroleptic iodonium complexes.<sup>17,18</sup> Secondly, all reported  $^{15}\text{N}$  NMR resonances of iodonium complexes manifest negative chemical shift changes, whilst the quinuclidine iodonium complexes synthesised herein were observed to have modestly reversed, *viz.* positive chemical shift changes, which highlights a drastic difference in the electronic environments of aromatic *versus* tertiary amine iodonium motifs.

Other solvent systems were attempted to further study the  $[1]^+$  series, such as DCM and DMSO, although these alternative solvent systems were largely unsuccessful for various reasons. When DCM was used as the solvent, it was found that during the preparation of the precursor  $[\text{Ag}(\text{quin})_2]^+$  complexes, DCM itself reacted. This side reaction gave rise to the dominant side product  $[\text{ClCH}_2(\text{quin})][\text{AgCl}_2]$ , in which quinuclidine had substituted a chlorine atom of DCM with the assistance of the  $\text{Ag}^+$  salt. DMSO, like MeCN, was found to be a suitable solvent for the reactions to proceed as desired; however, the resulting broadness of the  $^1\text{H}$  NMR spectra precluded the collection of satisfactory  $^1\text{H}$ - $^{15}\text{N}$  HMBC data, therefore preventing comparisons from being made regarding the values of the  $^{15}\text{N}$  NMR chemical shifts.

An examination of the solid-state structures of  $[1]\text{PF}_6$ ,  $[1]\text{NO}_3$ , and  $[1]\text{ClO}_4$  revealed that all I-N bond lengths were within a crystallographically indistinguishable (within a  $3\sigma^2$  tolerance) range of 2.293(4)–2.303(5) Å, although at the longer end of the range typically observed for N-heterocyclic iodonium complexes (2.23–2.32 Å),<sup>§</sup> and were actually more reminiscent of the bond lengths observed for iodonium complexes incorporating two sterically bulky groups at the *ortho*-positions, like with 2,4,6-trimethylpyridine ( $\sim 2.30$  Å).<sup>26,27</sup> A supra-molecular structure constructed from N–I–N linkages, based on the bicyclic tertiary amine DABCO (1,4-diazabicyclo[2.2.2]octane) as the coordinating group,<sup>15</sup> had I–N bond lengths in a

range of 2.25(2)–2.35(2) Å, which again is consistent with the values observed herein and for known N-heterocyclic iodonium complexes. The elemental iodine adduct of quinuclidine ( $\text{I}_2\text{-quin}$ ) was obtained as a trace impurity and its crystal structure has an I–N bond length of 2.35(1) Å, revealing that the quinuclidine ligands do bind to  $\text{I}^+$  more strongly than to neutral  $\text{I}_2$ . Given the cubic crystallographic symmetry of  $[1]\text{PF}_6$  and  $[1]\text{ClO}_4$ , only  $[1]\text{NO}_3$  (with an orthorhombic space group) has an N–I–N angle ( $179.6(2)^\circ$ ) that deviates from  $180^\circ$ , although  $[1]\text{PF}_6$  and  $[1]\text{NO}_3$  share a *staggered* conformation of the quinuclidine ligands (Fig. 2), contrary to the *eclipsed* conformation observed for  $[1]\text{ClO}_4$  (and previously reported for  $[1]\text{BF}_4$ ).<sup>13</sup> However, given that there is no  $\pi$ -system present as with the aromatic N-heterocyclic iodonium examples, these different orientations likely have no electronic significance and are simply a consequence of packing effects toward accommodating the various anions.

To further explore halonium complexes of tertiary amines, 1-ethylpiperidine (1-Etpip) was used as a ligand in an attempt to synthesise the analogous series of iodonium complexes  $[\text{I}(1\text{-Etpip})_2][\text{anion}]$  ( $[2][\text{anion}]$ ; anion =  $\text{BF}_4$ ,  $\text{PF}_6$ ,  $\text{NO}_3$ , and  $\text{ClO}_4$ ) as previously performed for quinuclidine. This monocyclic compound was seen as an ideal progression toward less strained tertiary amines compared to the rigid bicyclic quinuclidine, whilst effectively maintaining the steric and electronic properties for the purpose of comparison. However, in striking contrast to the stable  $[\text{I}(\text{quin})_2]^+$  complexes previously discussed, all complexes of  $[\text{I}(1\text{-Etpip})_2]^+$  were observed to immediately begin degrading upon synthesis, with complete decomposition of the iodonium complexes being observed (by  $^1\text{H}$  and  $^1\text{H}$ - $^{15}\text{N}$  HMBC NMR analyses) within 30 minutes from the addition of elemental iodine. Initially, this was believed to be due to the accessible pendant ethyl substituent, as the comparatively short longevity of  $[\text{I}(2\text{-ethylpyridine})_2]\text{PF}_6$  in solution has also recently been noted in comparison with its 4-ethylpyridine analogue,  $[\text{I}(4\text{-ethylpyridine})_2]\text{PF}_6$ .<sup>25</sup> However, given that iodonium complexes of 2,4,6-trimethylpyridine and  $[\text{I}(2\text{-ethylpyridine})_2]\text{PF}_6$  have been characterised in the solid state,<sup>26,27</sup> it would indicate that the pendant ethyl substituent is not solely the cause of the observed reactivity.

Complex  $[2]\text{NO}_3$  was observed to have the longest lifetime of the  $[2]^+$  complexes, with observation of the iodonium complex in the  $^1\text{H}$ - $^{15}\text{N}$  HMBC experiment being possible, and

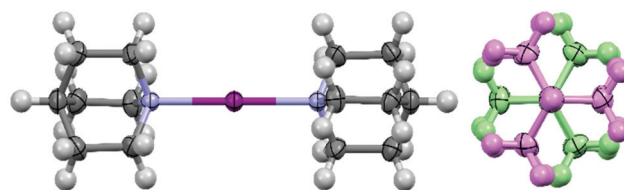


Fig. 2 The X-ray structure of  $[\text{I}(\text{quin})_2]^+$  from  $[1]\text{PF}_6$  (left), and viewed along the linear N–I–N bonds with the two quinuclidine ligands block coloured (right) highlighting their *staggered* conformation ( $\text{PF}_6$  anions omitted for clarity).



is therefore discussed as a representative of the series. As observed for the  $[1]^+$  complexes, upon complexation from 1-Et-pip to  $[2]NO_3$ , all resonances in the  $^1H$  NMR spectra were observed to shift to higher values by 0.74 ppm ( $\alpha$ -H), 0.29 ppm ( $\beta$ -H), 0.19 ppm ( $\gamma$ -H), 0.72 ppm ( $\delta$ -H), and 0.26 ppm ( $\epsilon$ -H) (Fig. 3). However, contrary to the positive shift observed in the  $^{15}N$  NMR resonances for the  $[1]^+$  complexes (*cf.* 9.3 ppm), upon complexation from 1-Et-pip ( $-329.4$  ppm) to  $[2]NO_3$  ( $-331.1$  ppm), a modest negative shift of  $-1.7$  ppm was observed, the directionality of which is in agreement with the change in the chemical shift seen for iodonium complexes comprised of aromatic N-heterocyclic ligands (*vide supra*), which also exhibit a negative shift. The  $^{15}N$  NMR chemical shift of  $[2]NO_3$  after 1 hour ( $-327.5$  ppm), however, revealed that the complex had completely decomposed to  $[H(1-Et-pip)]NO_3$  ( $-327.1$  ppm).

The vastly improved stability of the  $[1]^+$  complexes in comparison with  $[2]^+$  highlights the remarkable utility of bicyclic tertiary amines, such as quinuclidine, toward the formation of iodonium complexes. Therefore, the need to better comprehend the apparently unique electronic architecture of tertiary amine iodonium complexes is more crucial than ever and a worthwhile target for in-depth computational studies.

DFT calculations for  $[1]^+$ ,  $[2]^+$ , and (the previously reported)  $[I(DMAP)_2]^+$  iodonium complexes have been performed to rationalise the aforementioned electronic differences between aliphatic and aromatic amines. All complexes were optimised at the M06-2X/def2-TZVP level of theory (see ESI Computational methods<sup>†</sup>) and the resulting geometries are shown in Fig. 4 and 5. In agreement with the X-ray results, the I–N distances are longer for the aliphatic complexes  $[1]^+$  and  $[2]^+$  than for the  $[I(DMAP)_2]^+$  cation (see also Table 1). This gives reliability to the level of theory, which has already been used by us for the analysis of similar systems.<sup>1,24,25</sup> The natural population analysis (NPA) charges at the I atom are given in red in Fig. 4 and 5 (see also Table 1) and show that the iodine's positive charge is greater in the  $[I(DMAP)_2]^+$  cation than in  $[1]^+$  and  $[2]^+$ . This is counterintuitive taking into consideration that the I–N distance is shorter in  $[I(DMAP)_2]^+$ . A likely explanation is that in this complex some type of back-

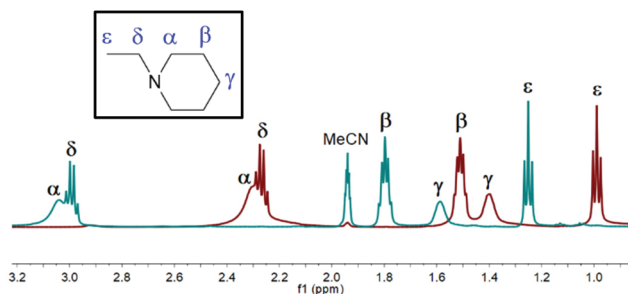


**Fig. 3** The superimposed  $^1H$  NMR spectra (500 MHz, 298 K) in  $CD_3CN$  of 1-ethylpiperidine (red) and  $[2]NO_3$  (turquoise) showing the observed shift upon formation of the iodonium complex. Inset: An annotated molecule of 1-ethylpiperidine.

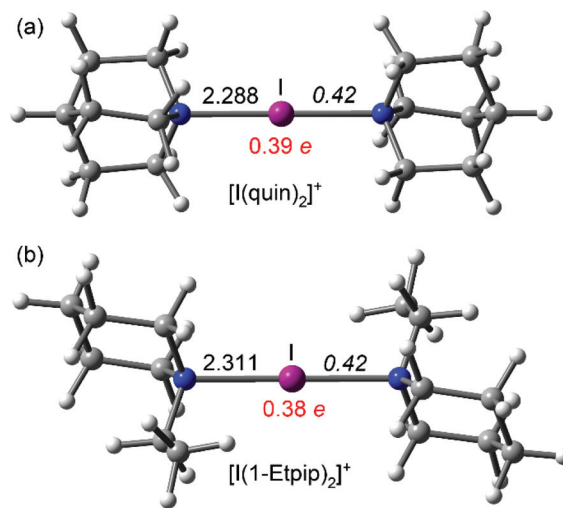


**Fig. 4** M06-2X/def2-TZVP optimised geometries of  $[1]^+$  (a) and  $[2]^+$  (b) (distances in Å; WBI in italics; and the NPA charge in red).

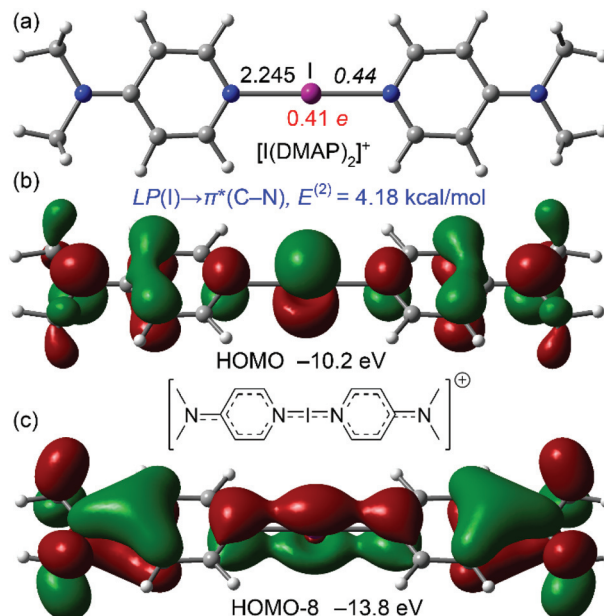


**Fig. 5** (a) M06-2X/def2-TZVP optimised geometry of  $[I(DMAP)_2]^+$  (distances in Å; WBI in italics; and the NPA charge in red). (b) HOMO representation. (c) HOMO–8 representation.

**Table 1** Dissociation energies ( $E_{dis}$ , kcal mol $^{-1}$ ), I–N distances ( $d$ , Å), WBI and NPA charges ( $e^-$ ) for  $[1]^+$ ,  $[2]^+$ , and  $[I(DMAP)_2]^+$  at the M06-2X/def2-TZVP level of theory

|           | $[1]^+$ | $[2]^+$ | $[I(DMAP)_2]^+$ |
|-----------|---------|---------|-----------------|
| $E_{dis}$ | 179.7   | 177.3   | 181.8           |
| $d$ (I–N) | 2.288   | 2.311   | 2.245           |
| NPA (I)   | 0.39    | 0.38    | 0.41            |
| WBI (I–N) | 0.42    | 0.42    | 0.44            |



donation from the iodine atom (free lone pair) to the  $\pi$ -system occurs. This phenomenon can explain the different behaviour of the aromatic compounds with respect to the aliphatic ones, affecting the aromatic ring current (NMR chemical shifts) and the stability of the complexes.

The Wiberg bond index (WBI) values are shown in italics in Fig. 4 and 5,<sup>28</sup> and support the proposed back-donation,  $I \rightarrow \pi(\text{py})$ , since the WBI value is larger (higher bond order) for the I–N bond in the  $[\text{I}(\text{DMAP})_2]^+$  cation, with the small difference indicating that the back-donation is small. Another interesting result that supports the back-donation is the orbital analysis of the complexes. Whilst complexes  $[1]^+$  and  $[2]^+$  only present  $\sigma$ -orbitals connecting the I and N atoms, the HOMO of the  $[\text{I}(\text{DMAP})_2]^+$  cation is  $\pi$ -type and exhibits an antibonding arrangement of the atomic N and I orbitals (Fig. 5). The corresponding bonding MO is much more stable (HOMO–8) and shows bonding overlap of the I and N atoms, thus evidencing a partial double bond character of the I–N bond, in agreement with the higher positive charge at the I atom (with a part of the electrons transferred to the pyridine  $\pi$ -system), the WBI value for the I–N bond, and shorter I–N bond lengths. Further evidence was also obtained from Natural Bond Orbital (NBO) analysis,<sup>29</sup> which showed a donor–acceptor interaction between the lone pair at the I atom and the antibonding C–N bonds of both pyridine rings, with a concomitant stabilisation energy of 4.18 kcal mol<sup>–1</sup>. Finally, the dissociation energies of the complexes have been computed (measured as  $[\text{IL}_2]^+ \rightarrow \text{I}^+ + 2\text{L}$ ;  $E_{\text{dis}}$ ). The results are presented in Table 1 and confirm the greatest stability of the  $[\text{I}(\text{DMAP})_2]^+$  complex followed by  $[1]^+$  and  $[2]^+$ , in line with the experimental results.

Whilst iodonium complexes have long enjoyed pride of place thanks to their myriad uses in organic transformations, their properties have still not been fully evaluated, which is especially true of iodonium complexes comprised of tertiary amines for which there are very few examples. The work herein has extensively studied iodonium complexes of comparable bicyclic and monocyclic tertiary amines, and highlights that the stability of bicyclic tertiary amines is exceptional, although monocyclic complexes can also be synthesised despite their increased reactivity. The structural studies of the  $[1]^+$  series of complexes have revealed that, despite the electronic differences, the complexes are remarkably reminiscent of their aromatic counterparts, such as  $[\text{I}(\text{DMAP})_2]^+$ , with respect to the I–N bond lengths.

The electronic structures of tertiary amine iodonium complexes may lack some of the favourable interactions of their aromatic analogues, such as stabilising  $\pi$ -interactions; however, experimental and theoretical studies reveal that the resulting iodonium complexes still possess many of the same features, despite the diminished longevity that was observed for the  $[2]^+$  series of complexes.

## Conflicts of interest

There are no conflicts to declare.

## Acknowledgements

We gratefully acknowledge the Finnish Cultural Foundation Central Fund (J. S. W.; grant number 00201148), the Magnus Ehrnrooth Foundation (J. S. W.), the MICIU/AEI of Spain (A. F.; project CTQ2017-85821-R FEDER), the Academy of Finland (K. R.; grant no. 317259), and the University of Jyväskylä, Finland, for financial support.

## Notes and references

‡ $[\text{I}(\text{triethanolamine})_2]\text{I}$  has been reported previously;<sup>30</sup> however, the authors could not independently confirm this work as only the unit cell was provided in the CSD (TEAMID10; no atomic coordinates were included). Therefore, this work cannot be discussed herein.

§Based on the search of the CSD for the I–N bond lengths for all reported N-heterocyclic iodonium complexes.

- 1 S. Yu, P. Kumar, J. S. Ward, A. Frontera and K. Rissanen, *Chem*, 2021, **7**, 948–958.
- 2 J. A. Creighton, I. Haque and J. L. Wood, *Chem. Commun.*, 1966, 229.
- 3 I. Haque and J. L. Wood, *J. Mol. Struct.*, 1968, **2**, 217–238.
- 4 G. Cavallo, P. Metrangolo, R. Milani, T. Pilati, A. Priimagi, G. Resnati and G. Terraneo, *Chem. Rev.*, 2016, **116**, 2478–2601.
- 5 J. Barluenga, J. M. González, M. A. Garcia-Martin, P. J. Campos and G. Asensio, *J. Chem. Soc., Chem. Commun.*, 1992, 1016–1017.
- 6 J. Ezquerra, C. Pedregal, C. Lamas, J. Barluenga, M. Pérez, M. A. García-Martín and J. M. González, *J. Org. Chem.*, 1996, **61**, 5804–5812.
- 7 G. Espuña, G. Arsequell, G. Valencia, J. Barluenga, M. Pérez and J. M. González, *Chem. Commun.*, 2000, 1307–1308.
- 8 L. Turunen and M. Erdélyi, *Chem. Soc. Rev.*, 2020, **49**, 2688–2700.
- 9 G. A. Bowmaker and S. F. Hannan, *Aust. J. Chem.*, 1971, **24**, 2237–2248.
- 10 H. Pritzkow, *Acta Crystallogr., Sect. B: Struct. Crystallogr. Cryst. Chem.*, 1975, **31**, 1505–1506.
- 11 H. Hartl and M. Hedrich, *Z. Naturforsch., B: Anorg. Chem., Org. Chem., Biochem., Biophys., Biol.*, 1981, **36b**, 922–928.
- 12 L. K. Blair, K. D. Parris, P. Sen Hii and C. P. Brock, *J. Am. Chem. Soc.*, 1983, **105**, 3649–3653.
- 13 C. P. Brock, Y. Fu, L. K. Blair, P. Chen and M. Lovell, *Acta Crystallogr., Sect. C: Cryst. Struct. Commun.*, 1988, **44**, 1582–1585.
- 14 Y.-M. Wang, J. Wu, C. Hoong, V. Rauniyar and F. D. Toste, *J. Am. Chem. Soc.*, 2012, **134**, 12928–12931.
- 15 L. Turunen, A. Peuronen, S. Forsblom, E. Kalenius, M. Lahtinen and K. Rissanen, *Chem. – Eur. J.*, 2017, **23**, 11714–11718.
- 16 C. Weinberger, R. Hines, M. Zeller and S. V. Rosokha, *Chem. Commun.*, 2018, **54**, 8060–8063.
- 17 S. Lindblad, K. Mehmeti, A. X. Veiga, B. Nekoueishahraki, J. Gräfenstein and M. Erdélyi, *J. Am. Chem. Soc.*, 2018, **140**, 13503–13513.
- 18 J. S. Ward, G. Fiorini, A. Frontera and K. Rissanen, *Chem. Commun.*, 2020, **56**, 8428–8431.



- 19 D. von der Heiden, K. Rissanen and M. Erdélyi, *Chem. Commun.*, 2020, **56**, 14431–14434.
- 20 L. Turunen, U. Warzok, R. Puttreddy, N. K. Beyeh, C. A. Schalley and K. Rissanen, *Angew. Chem., Int. Ed.*, 2016, **55**, 14033–14036.
- 21 L. Turunen, U. Warzok, C. A. Schalley and K. Rissanen, *Chem*, 2017, **3**, 861–869.
- 22 U. Warzok, M. Marianski, W. Hoffmann, L. Turunen, K. Rissanen, K. Pagel and C. A. Schalley, *Chem. Sci.*, 2018, **9**, 8343–8351.
- 23 A. Vanderkooy, A. K. Gupta, T. Földes, S. Lindblad, A. Orthaber, I. Pápai and M. Erdélyi, *Angew. Chem., Int. Ed.*, 2019, **58**, 9012–9016.
- 24 J. S. Ward, A. Frontera and K. Rissanen, *Inorg. Chem.*, 2021, **60**, 5383–5390.
- 25 J. S. Ward, A. Frontera and K. Rissanen, *Chem. Commun.*, 2021, **57**(41), 5094–5097.
- 26 T. Okitsu, S. Yumitate, K. Sato, Y. In and A. Wada, *Chem. – Eur. J.*, 2013, **19**, 4992–4996.
- 27 L. C. F. Morgan, Y. Kim, J. N. Blandy, C. A. Murray, K. E. Christensen and A. L. Thompson, *Chem. Commun.*, 2018, **54**, 9849–9852.
- 28 K. B. Wiberg, *Tetrahedron*, 1968, **24**, 1083–1096.
- 29 E. D. Glendening, C. R. Landis and F. Weinhold, *Wiley Interdiscip. Rev.: Comput. Mol. Sci.*, 2012, **2**, 1–42.
- 30 C. Wyganowski, *Pol. J. Chem.*, 1978, **52**, 203.

